Antitumor Activity of a Small-Molecule Inhibitor of Human Silent Information Regulator 2 Enzymes

Birgit Heltweg,[1] Tonibelle Gatbonton,[1] Aaron D. Schuler,[1,2] Jeff Posakony,[1,2] Hongzhe Li,[4] Sondra Goehle,[1] Ramya Kollipara,[5] Ronald A. DePinho,[5] Yansong Gu,[4] Julian A. Simon,[1,2] and Antonio Bedalov[1,3]

[1]Clinical Research and [2]Human Biology Divisions, Fred Hutchinson Cancer Research Center; Departments of [3]Medicine and [4]Radiation Oncology and Immunology, University of Washington, Seattle, Washington; and [5]Department of Medical Oncology, Dana-Farber Cancer Institute, Departments of Medicine and Genetics, Harvard Medical School, Boston, Massachusetts

Abstract

SIRT1 and other NAD-dependent deacetylases have been implicated in control of cellular responses to stress and in tumorigenesis through deacetylation of important regulatory proteins, including p53 and the BCL6 oncoprotein. Hereby, we describe the identification of a compound we named cambinol that inhibits NAD-dependent deacetylase activity of human SIRT1 and SIRT2. Consistent with the role of SIRT1 in promoting cell survival during stress, inhibition of SIRT1 activity with cambinol during genotoxic stress leads to hyperacetylation of key stress response proteins and promotes cell cycle arrest. Treatment of BCL6-expressing Burkitt lymphoma cells with cambinol as a single agent induced apoptosis, which was accompanied by hyperacetylation of BCL6 and p53. Because acetylation inactivates BCL6 and has the opposite effect on the function of p53 and other checkpoint pathways, the antitumor activity of cambinol in Burkitt lymphoma cells may be accomplished through a combined effect of BCL6 inactivation and checkpoint activation. Cambinol was well tolerated in mice and inhibited growth of Burkitt lymphoma xenografts. Inhibitors of NAD-dependent deacetylases may constitute novel anticancer agents. (Cancer Res 2006; 66(8): 4368-77)

Introduction

Reversible protein acetylation is an important posttranslational modification that regulates the function of histones and many other proteins (1). Acetylation of lysine residues, carried out by histone/protein acetyltransferases (e.g., p300, CBP, and p/CAF in mammalian cells), is counteracted by the activity of histone deacetylases (HDAC), which remove acetyl groups from the same targets. Based on the similarity of their primary structures, HDACs can be divided into three groups (2). Class I and II HDACs (classic HDACs) use a Zn^{2+} ion at the active site to activate a water molecule for amide bond hydrolysis. Class III HDACs or Sir2 family of enzymes catalyze a different reaction in which the removal of the acetyl group from the lysine residues is coupled with the hydrolysis of NAD to generate nicotinamide, lysine, and *O*-acetyl-ADP-ribose (3, 4). Although the details of this unique biochemical reaction are not yet fully understood at the molecular level, crystal structures of several members of the family have revealed that NAD and the acetylated peptide bind to distinct domains of the protein (5–8). NAD binding is accomplished through a protein domain previously characterized as a NAD(H) binding domain in dehydrogenases called the Rossman fold, whereas peptide binding occurs in the cleft adjacent to a small helical domain.

The Sir2 family of enzymes, broadly conserved through organisms ranging from bacteria to humans, has been implicated in a wide range of biological processes, including genetic control of aging in yeast, nematodes, and flies; development in flies and mice; and in control of intermediary metabolisms in bacteria (reviewed in refs. 9, 10). Humans have seven different NAD-dependent deacetylase genes, *SIRT1* to *SIRT7* (11). SIRT1 is a nuclear enzyme that deacetylates histones and several nonhistone proteins. Additionally, SIRT1 and other sirtuins were found to regulate cell survival during stress through deacetylation of key cell cycle and apoptosis regulatory proteins, including p53 (12, 13), Ku70 (14), and forkhead transcription factors (15). Acetylation of p53, Foxo3a, and Ku70 brought about through stress-induced activation of cellular histone/protein acetyltransferases promotes cell death and this effect is counteracted by sirtuin-mediated deacetylation of these protein targets. SIRT1-mediated deacetylation of p53 and Foxo3a interferes with their transactivating functions and deacetylation of Ku70 enhances its binding to the proapoptotic Bax protein, which sequesters and thus inactivates Bax (14). Related to these cell survival functions, SIRT1 was also shown to play a role in prevention of axonal degeneration (16) and in mediating calorie restriction–induced stress resistance in rodents (17). Silent information regulator 2 (Sir2)–like enzymes in mammals have also been implicated in differentiation of several tissues, including B lymphocytes, through deacetylation of the transcriptional repressor BCL6 (18), skeletal muscle through deacetylation of transcription factor MyoD (19), and in adipogenesis through interactions with peroxisome proliferator activated receptor γ (20). Less is known about the functions of other mammalian sirtuins. SIRT2 is primarily a cytoplasmic protein that deacetylates tubulin (21) and SIRT3 is a mitochondrial enzyme whose function and protein targets are not known (22).

Although structurally and mechanistically unrelated, sirtuins (class III HDACs) and classic HDACs (class I and II deacetylases) share many common protein targets as exemplified by several of the discussed proteins (e.g., p53, Ku70, BCL6, and tubulin; refs. 18, 23, 24). Inhibitors of classic HDACs (e.g., depsipeptide, SAHA) have potent antitumor activity (25–27) consistent with the important

Note: Supplementary data for this article are available at Cancer Research Online (http://cancerres.aacrjournals.org/).

A. Bedalov is Ellison Medical Foundation Scholar. B. Heltweg is a DeutscheForschungsgemeinschaft recipient.

Requests for reprints: Antonio Bedalov, Clinical Research Division, Fred Hutchinson Cancer Research Center, D2-100, 1100 Fairview Avenue North, Seattle WA 98109. Phone: 206-667-4863; Fax: 206-667-5669; E-mail: abedalov@fhcrc.org.

doi:10.1158/0008-5472.CAN-05-3617

role of protein acetylation in tumorigenesis. Given the antitumor activity of inhibitors of classic HDACs and the known SIRT1 role in deacetylation of proteins that regulate cell survival during stress (e.g., p53, KU70, and Foxo3a) and oncogenesis (e.g., BCL6), we decided to explore the possibility that pharmacologic inhibition of NAD-dependent deacetylases could be used as an anticancer strategy. The demonstration that complete absence of SIRT1 is compatible with both cell and animal viability in mouse SIRT1 knockout studies (28, 29) suggests that pharmacologic inhibition of SIRT1 deacetylase for therapeutic purposes may be well tolerated by normal tissues.

We have previously identified splitomicin (Fig. 1*A*; ref. 30), a potent inhibitor of NAD-dependent HDACs, through a yeast cell-based screen for inhibitors of telomeric silencing. Splitomicin and its derivatives inhibit Sir2 and Sir2 homologues in yeast *in vivo* (30–33). However, the hydrolysis of splitomicin and related lactone compounds at neutral pH (i.e., half-life 30 minutes at pH 7.4; ref. 34) complicates their use in mammalian cells. Hereby, we report the identification and characterization of chemically stable compound related to splitomicin, which we named cambinol, that inhibits the activity of human SIRT1 and SIRT2 and that exerts antitumor activity *in vitro* and in mouse xenograft studies.

Materials and Methods

Reagents and antibodies. NSC-112546, here called cambinol, was obtained from the National Cancer Institute (NCI) repository of drugs. Splitomicin was identified in yeast cell–based screen for inhibitors of telomeric silencing (30). The screen of NCI compounds yielded one strongly positive hit labeled NSC-112546. Chemical analysis of the contents of this well revealed that NSC-112546 is actually a mixture of three compounds. The most abundant component is cambinol (identified in the NCI/Developmental Therapeutics Program database as NSC-112546). The next most abundant component is splitomicin, which is a by-product in the synthesis of NSC-112546 (cambinol). Finally, the mixture also contains the hydrolysis product of splitomicin (2-hydroxy-1-[3′-propionyl]-naphthalene). All of these compounds, as well as ADS012, were synthesized, purified to homogeneity, and tested for activity in cell-based and *in vitro* assays. Trichostatin A, nicotinamide, etoposide, and paclitaxel were purchased from Sigma. Antibodies to acetylated α-tubulin (clone 6-11B-1, Sigma, St. Louis, MO), α-tubulin (clone DM1A, Calbiochem, San Diego, CA), actin (Roche, Indianapolis, IN), acetylated p53 (Cell Signaling, Danvers, MA), acetylated lysine (polyclonal antibody; Cell Signaling), BCL6 (N-3, for Western blotting; Santa Cruz Biotechnology, Santa Cruz, CA), BCL6 (PG-6Bp, for immunoprecipitation; DAKOCytomation, Carpinteria, CA), Ku70 (C-19, for Western blotting and immunoprecipitation; Santa Cruz), p53 (Ab-6; Calbiochem), and SIRT1 (Santa Cruz Biotechnology) were commercially obtained.

HDAC assay. The HDAC assay was done using bacterially expressed and purified glutathione *S*-transferase (GST) fusion proteins as previously described (33). The GST-SIRT2 expression plasmid was a gift of Dr. D. Moazed (Department of Cell Biology, Harvard Medical School, Boston, MA) (35). SIRT1, SIRT3, and SIRT5 cDNA were generously provided by Dr. E. Verdin (Gladstone Institute of Virology and Immunology, San Francisco, CA) (21). The genes were cloned into GST expression plasmids, expressed, and purified in bacteria. For deacetylation assays, chemically acetylated [^{3}H]acetyl-H4 peptide (33) was incubated with or without 500 μmol/L NAD^+, 0.1 μg GST enzyme in the buffer containing 150 mmol/L NAD, 50 mmol/L Tris-HCl (pH 8.0), 1 mmol/L DTT, and 5% glycerol. After 3 hours of incubation at 37°C for SIRT1, SIRT2, SIRT3, and overnight incubation for SIRT5 (at 37°C), the reaction was quenched by the addition of 5 μL of 1 N HCl with 0.15 N acetic acid. Released [^{3}H]acetic acid was extracted with 400 μL ethyl acetate and counted in 5 mL scintillation fluid. HDAC6 obtained from HeLa cells was transfected with HDAC6 expression plasmid by immunoprecipitation. HDAC6-specific rabbit polyclonal antibody and HDAC6 expression vector were a gift from Bob Eisenman (Fred Hutchinson Cancer Research Center).

Cell culture. All cells were maintained at 37°C and 5% CO_2; the appropriate medium was supplemented with 1% L-glutamine (Life Technologies, Carlsbad, CA) and 1% penicillin-streptomycin (Life Technologies).

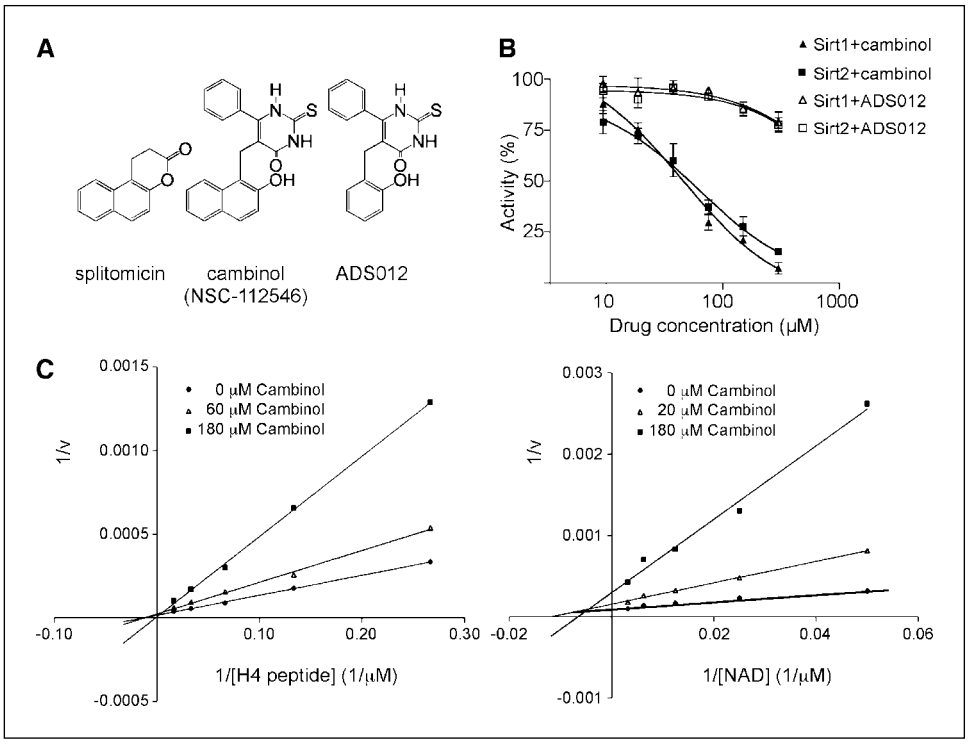

Figure 1. Sirtuin inhibitors. *A,* structure of splitomicin, cambinol (NSC-112546), and ADS012. *B,* cambinol inhibits human SIRT1 (IC_{50}, 56 ± 2 μmol/L) and SIRT2 (IC_{50}, 59 ± 4) NAD-dependent deacetylation of acetyl-histone H4 peptide. Napthol to phenol substitution in ADS012 leads to loss of SIRT1 and SIRT2 inhibition. *Y axis,* relative NAD-dependent deacetylase activity. *C,* cambinol exhibits competitive inhibition toward acetyl-histone H4 peptide (*left*) and noncompetitive inhibition toward NAD (*right*) in the SIRT2-catalyzed reaction. *Left,* double-reciprocal plots of 1 / *v* versus 1 / [acetyl-H4 peptide]. Concentrations of acetyl-H4 peptide ranged from 3.7 to 60 μmol/L in the presence of 500 μmol/L NAD and the indicated concentrations of cambinol. The intersection of the lines at the 1 / *v* axis indicates competitive inhibition. *Right,* double-reciprocal plots of 1 / *v* versus 1 / [NAD]. The concentrations of NAD ranged from 20 to 360 μmol/L in the presence of 20 μmol/L acetyl-histone H4 peptide and the indicated concentrations of cambinol. The intersection of the lines left of the 1 / *v* axis and above the 1 / [NAD] axis indicates noncompetitive inhibition. All data points were examined in triplicates and were fitted to double reciprocal plots using the Prism software. *Y axis,* 1 / *v* ($hcpm^{-1}$).

The nonadherent cell lines Dakiki, Daudi, Mutu1, Namalwa, Oku1, and Ramos were cultured in RPMI supplemented with 20% FCS. The EBV-transformed normal B cells B1, B2, and B3 and the cancer cells NCI H460 and Ovcar-3 were cultured in RPMI plus 10% FCS. HCT116, human foreskin fibroblasts, MCF-ADR, mouse embryonic fibroblasts (MEF) F61 and F80, 293/Phoenix, UACC 62, and Rat1a were maintained in DMEM plus 10% FCS. The chicken cells DT40 were grown in RPMI supplemented with 10% FCS, 1% chicken serum, and 10 μmol/L 2-mercaptoethanol. MCF-7 cells were maintained in DMEM with 10% FCS, 1% MEM nonessential amino acids (Life Technologies), 1% MEM sodium pyruvate (Life Technologies), 1 μg/mL human insulin (Life Technologies), 1 μg/mL hydrocortisone (Sigma), and 1 ng/mL human epidermal growth factor (Life Technologies) buffered with HEPES.

Daudi, Dakiki, Namalwa, Ramos, HCT116, and NCI-H460 cells were obtained from American Type Culture Collection (Manassas, VA). The Burkitt lymphoma cells Oku1 and Mutu1 were received from Dr. I. Ruf (St. Jude Children's Research Hospital, Memphis, TN). The chicken cell lines DT40 cl18 and DT40 no. 77 were obtained from S. Takeda (CREST, Japan Science and Technology, Kyoto University, Kyoto, Japan). The normal B cell lines B1, B2, and B3 were EBV-transformed B cells obtained from Dr. Banker (Fred Hutchinson Cancer Research Center). The matched MEF F61 and F80 were received from Dr. Sanchez (Fred Hutchinson Cancer Research Center). Foxo3a MEF fibroblasts were generated from Foxo3a knockout mice (36).

BCL6 transcriptional reporter assay. The components of previously described (37) BCL6 transcriptional reporter system consisting of luciferase reporter gene under control of thymidine kinase promoter and five GAL4 binding sites (G5TK-pGL2) and the expression vector for a fusion protein that contains Gal4 DNA binding domain fused to BCL6 pCDA3(GAL4)-BCL6 were obtained from Dr. Paul Wade (Emory University, Atlanta, GA). The reporter construct with or without varying amounts of GAL4-BCL6 expression plasmid were introduced into NCI-H460 cells using calcium phosphate method. A plasmid containing cytomegalovirus (CMV)-driven β-galactosidase reporter (50 ng) was cotransfected to control for transfection efficiency. Sixteen hours after transfection, cells were treated with 100 μmol/L cambinol of DMSO (control) for 24 hours and the luciferase and β-galactosidase activity was measured.

Immunoprecipitations and Western blot analysis. Cells were treated with the drugs for 16 or 5 hours for Burkitt lymphoma cell lines Ramos and Namalwa, lysed in a buffer containing 20 mmol/L Tris-HCl (pH 7.5), 150 mmol/L NaCl, 1 mmol/L EDTA, 1 mmol/L EGTA, 1% Triton X-100, 2.5 mmol/L sodium PPi, 1 mmol/L glycerophosphate, 1 mmol/L orthovanadate, 1 mmol/L phenylmethylsulfonyl fluoride (PMSF), 0.66 μmol/L trichostatin A, and 10 mmol/L nicotinamide in the presence of Complete Mini protease inhibitors (Roche). For immunoprecipitation, lysates were precleared for 30 minutes with Gammabind Plus beads (Amersham Pharmacia Biotech, Piscataway, NJ) at 4°C. Primary antibodies were added and the lysates were rocked at 4°C for 2 hours. Immunocomplexes were captured by the addition of Gammabind Plus beads and rocked for another 2 hours at 4°C. The beads were washed four times with lysis buffer, 2× SDS loading buffer was added, and the proteins were eluted by boiling for 5 minutes. For the detection of BCL6, 4×10^6 Ramos cells were treated with drugs for 5 hours and lysed with radioimmunoprecipitation assay buffer [50 mmol/L Tris (pH 8.0), 250 mmol/L NaCl, 1% NP40, 0.5% deoxycholic acid, 0.1% SDS, Complete Mini protease inhibitors, 1 μmol/L trichostatin A, and 10 mmol/L nicotinamide]. Before immunoprecipitation, lysates were diluted 1:3 with NP40 buffer [50 mmol/L Tris-HCl (pH 8.0), 150 mmol/L NaCl, 0.1% NP40, 10% glycerol, 5 mmol/L $MgCl_2$, 1 mmol/L DTT, 2.5 mmol/L sodium PPi, 10 mmol/L glycerophosphate, 1 mmol/L orthovanadate, 1 mmol/L PMSF, Complete Mini protease inhibitors, 1 μmol/L trichostatin A, and 5 mmol/L nicotinamide]. Cell lysates or immunoprecipitates were resolved by SDS-PAGE in 10% polyacrylamide gels and transferred onto nitrocellulose membranes. Proteins were visualized using SuperSignal West Pico Chemiluminescent Substrate (Pierce, Rockford, IL).

Immunofluorescence. NCI H460 cells grown on coverslips for 24 hours were treated with 100 μmol/L cambinol and 2.5 nmol/L trichostatin A (Sigma) for another 16 hours. Cells were permeabilized with 0.5% Triton X-100 in warm microtubule stabilizing buffer [80 mmol/L PIPES (pH 6.8), 1 mmol/L $MgCl_2$, and 5 mmol/L EGTA] and fixed with glutaraldehyde for 10 minutes. Primary antibodies were targeted against α-tubulin (clone DM1A, Calbiochem) and acetylated α-tubulin (clone 6-11B-1, Sigma). Oregon green–conjugated anti-mouse IgG (Molecular Probes, Carlsbad, CA) was used as secondary antibody. Slides were visualized on a Nikon E800 microscope system equipped with a SPOT2 digital camera.

Toxicity assays. Toxicity was measured with a modified [^{3}H]thymidine incorporation assay as described previously (38). In brief, cells plated in a 96-well microplate were treated with drugs for 96 hours (4 days) after which medium with the drug was removed and fresh medium containing [^{3}H]thymidine was added. Twenty-four hours later, the medium with [^{3}H]thymidine was removed and [^{3}H]thymidine incorporation was measured. Each drug concentration was tested in triplicate. For synergy experiments, the viability of cells treated with two drugs was normalized to the viability of cells that were treated with a single drug. Synergy was evaluated by comparing the IC_{50} values of the particular drug with and without cambinol and the P values were obtained using the Student's t test and was confirmed independently using the method of isobole (39).

Cell cycle analysis. Propidium iodide staining of whole cells was analyzed by flow cytometry. A minimum of 10,000 cells were analyzed for each sample, and results are representative of at least two independent experiments. Cells were treated with the drugs for 48 hours. Both adherent and floating cells were collected, washed with PBS, supplemented with 1% FCS, and fixed with 80% ethanol at 4°C. After washing with PBS, cells were permeabilized with 0.25% Triton X-100 for 5 minutes, washed, and stained in propidium iodide solution in PBS (10 μg/mL propidium iodide and 1 mg/mL RNase) for 30 minutes at 37°C. The DNA fluorescence was measured by using a FACScanR (Becton Dickinson, Franklin Lakes, NJ) and data analysis was done using FlowJo software.

RNA interference. For small interfering RNA experiments, we generated a pBabe-based retroviral vector expressing a hairpin RNA from the human H1 promoter cloned into the second long terminal repeat. The sequence CAGGTTGCGGGAATCCAAA targets human SIRT1. For retroviral infections, amphotropic virus was made from 293/Phoenix cells by transient transfection of pBabe plasmids. One milliliter of viral supernatant was mixed with 1 mL fresh medium to infect NCI H460 cells (60 mm dishes) overnight. This was repeated once after 24 hours. Twenty-four hours after the last infection, the cell supernatant was changed to fresh growth medium. Forty-eight hours after the last infection, stably infected cells were selected with puromycin (2.5 μg/mL) for 1 week.

Retroviral infection in Burkitt lymphoma cells. Retroviral expression vectors PINCO, PINCO-BCL6, and PINCO-HA-BCL6ΔPEST (40, 41), obtained from R. Della-Favera (Columbia University, New York, NY), were introduced into 293/Phoenix packaging cell line by transient transfection using the calcium phosphate method as described in http://www.stanford.edu/group/nolan/retroviral_systems/phx.html. For infection, 2 million Namalwa cells were resuspended in 2 mL of 50:50 mixture of the viral supernatant and the usual medium [Iscove's modified Dulbecco's medium (IMDM) supplemented with 20% FCS] with 5 μg/mL polybrene, centrifuged for 1 hour at 1,800 rpm, and incubated at 37°C overnight. After removal of the old medium by careful aspiration (without moving cell out of plates), the same procedure is repeated again the following day. One day after second round of infection, polybrene/retroviral supernatant is removed and replaced with fresh medium (IMDM supplemented with 20% FCS). After 3 days, green fluorescent protein–positive (GFP+) cells (10-15% of total cells) were selected using VANTAGE Cell Sorter (Becton Dickinson). GFP+ cell populations were expanded over 72 hours and characterized by Western blot analysis for HA-BCL6 expression using antihemagglutinin antibody and sensitivity to cambinol using the [^{3}H]thymidine incorporation assay in a 96-well format.

Animal xenograft studies. Daudi Burkitt lymphoma cells (20×10^6) resuspended in PBS were administered s.c. into the flank of 6- to 8-week-old nonobese diabetic/severe combined immunodeficient male mice. Palpable tumors arose in 100% of the animals after a median of 3 to 4 days.

Cambinol, prepared as 10%/10% ethanol/Cremophore solution to improve solubility, at the dose of 100 mg/kg, or vehicle were administered i.v. through tail vein injection or i.p. daily from day 5 to 19 (five injections per week). The dose of 100 mg/kg cambinol was the highest dose that could be administered as a single i.v. injection due to limited solubility of the drug. Tumor size was measured thrice a week using caliper and the tumor volumes were calculated.

Results

In the search for chemically stable sirtuin inhibitors, we identified a β-naphthol compound, cambinol (Fig. 1*A*), that inhibits human SIRT1 and SIRT2 NAD-dependent deacetylase activity *in vitro* with IC_{50} values of 56 and 59 μmol/L, respectively (Fig. 1*B*). Cambinol had only weak inhibitory activity against SIRT5 (42% inhibition at 300 μmol/L) and no activity against SIRT3 (Supplementary Fig. S1). SIRT4, SIRT6, and SIRT7 do not possess *in vitro* deacetylase activity (21). Class I and II HDACs were not affected by cambinol as determined by the examination of the effect of cambinol on nuclear or cytoplasmic (HDAC6) deacetylases (Supplementary Figs. S2 and S3). The substitution of β-naphtol in cambinol with phenol (compound ADS012; Fig. 1*A*) led to loss of inhibitory activity against both SIRT1 and SIRT2 (Fig. 1*B*) consistent with the importance of β-naphtol pharmacophore for the antisirtuin activity of cambinol. SIRT2 competition studies with NAD and histone H4-peptide substrates revealed that cambinol is competitive with the peptide and noncompetitive with NAD (Fig. 1*C*). The fact that cambinol does not affect NAD binding to sirtuins suggests that cambinol is unlikely to interfere with NAD binding in other Rossman-fold-containing enzymes, which includes a large number of cellular dehydrogenases.

Cambinol-mediated inhibition of cellular sirtuins leads to hyperacetylation of tubulin, p53, and other SIRT1 and SIRT2 deacetylation targets. To show that cambinol inhibits the activity of cellular sirtuins, we examined the acetylation status of several known SIRT1 and SIRT2 deacetylation targets after cambinol treatment, including tubulin and p53. The deacetylation of the ε-amino group of α-tubulin Lys^{40} is carried out by both a sirtuin, SIRT2 (21), and a class II HDAC, HDAC6 (42). A highly specific monoclonal antibody (clone 6-11B-1) is available for monitoring of this protein modification (43). We analyzed the effect of cambinol on tubulin acetylation in NCI H460 lung cancer cell line using indirect immunofluorescence and immunoblotting techniques (Fig. 2*A* and *B*). Treatment with the HDAC6 inhibitor trichostatin A or the SIRT2 inhibitor cambinol alone did not significantly alter the acetylation status of tubulin. (Low dose of trichostatin A, which does not induce appreciable acetylation effect when trichostatin A is used alone, has been chosen in these studies so that the effect of SIRT2 inhibition on tubulin acetylation can be more easily appreciated.) However, combined inhibition of both enzymes resulted in hyperacetylation of tubulin. This result is consistent with the shared roles of the HDACs and sirtuins in tubulin deacetylation and it shows that cambinol inhibits deacetylase activity of SIRT2 *in vivo*.

Next, we studied the acetylation status of p53, a known SIRT1 substrate, after treatment with cambinol. As SIRT1 has been shown to deacetylate p53 on DNA damage, we evaluated whether inhibition of SIRT1 with cambinol increases acetylation of p53 in NCI H460 cells after etoposide-inflicted DNA damage. NCI H460 cells, which have intact p53, were treated with etoposide, trichostatin A, cambinol, or combinations of the three drugs and analyzed by immunoblotting using acetyl-p53 and p53-specific antibodies. As expected, etoposide treatment increased total p53 protein levels (Fig. 2*C*). Furthermore, a barely detectable acetyl-p53 was also observed in etoposide-treated cells, consistent with DNA damage–induced activation of p53 protein by acetylation (13). However, the combined treatment of cells with

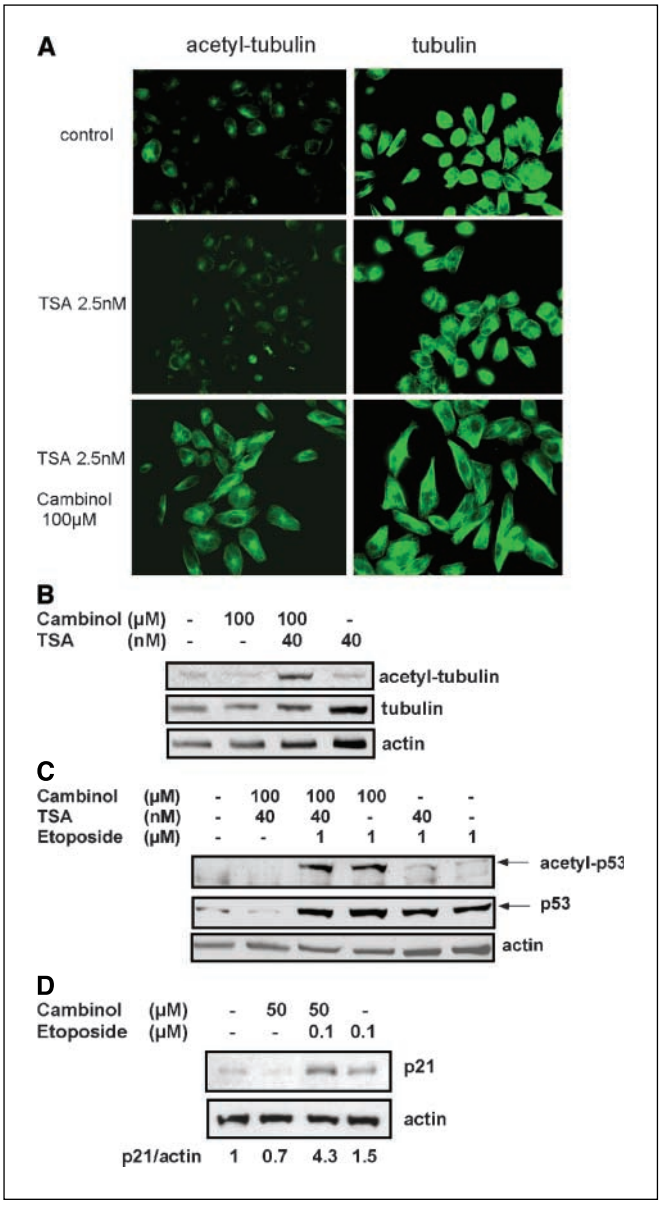

Figure 2. Cambinol induces hyperacetylation of SIRT1 and SIRT2 substrates p53 and tubulin. *A,* acetyl-tubulin immunoflorescence. NCI H460 cells were grown on coverslips and treated with the indicated concentrations of the HDAC6 inhibitor trichostatin A (*TSA*) and with the SIRT2 inhibitor cambinol for 16 hours. Acetylated α-tubulin and α-tubulin were visualized by indirect immunofluorescence. *B,* acetyl-tubulin immunoblot. NCI H460 cells were treated with indicated drugs for 16 hours. Tubulin and actin immunoblots are shown as loading controls. *C,* cambinol induces hyperacetylation of p53 following DNA damage. NCI H460 were treated with the indicated concentration of etoposide and the deacetylase inhibitors (cambinol and trichostatin A) for 16 hours. *Top,* acetylated p53. *Middle,* total p53; *Bottom,* actin immunoblot provided as loading control. *D,* cambinol stimulates etoposide-mediated induction of p21. Cells were treated with the indicated concentrations of drugs for 8 hours and the cell lysates were analyzed by immunoblots using anti-p21 and anti-actin (loading control) antibodies. Normalized p21/actin ratio is determined by densitometry.

etoposide and cambinol led to a significant increase in p53 acetylation. This result shows that cambinol inhibits SIRT1 deacetylase activity *in vivo* and it suggests that the treatment of cells with cambinol stimulates p53 activation on DNA damage. To evaluate whether cambinol increased p53 activation, we examined induction of *p21*, a known p53 target gene, during DNA damage response. Consistent with increased activation of p53, we found that cambinol promoted etoposide-induced p21 induction (Fig. 2*D*).

In addition to p53, SIRT1 and other sirtuins have been implicated in the deacetylation of Ku70 (15) and forkhead transcription factor Foxo3a (15). Deacetylation of these proteins promotes survival during stress. Ku70 and Foxo3a immunoprecipitation experiments from HeLa cells treated with the deacetylase inhibitors trichostatin A and cambinol show that inhibition of cellular sirtuins with cambinol leads to Ku70 and Foxo3a hyperacetylation (Supplementary Fig. S4). Together, these results suggest that inhibition of SIRT1 with cambinol abrogates several sirtuin-dependent cellular survival pathways.

Cambinol-mediated inhibition of SIRT1 sensitizes cells to DNA-damaging agents in p53-independent manner. Because we have shown that cambinol-mediated inhibition of SIRT1 increases acetylation of p53, Ku70, and Foxo3a, we evaluated whether cambinol treatment could sensitize cell to DNA-damaging agent etoposide. We first tested p53-positive lung cancer cell line NCI H460. As expected from the p53 acetylation studies in NCI H460 cells, we found that cambinol induced dose-dependent sensitization to etoposide (Fig. 3*A*). Down-regulation of the endogenous SIRT1 protein level in NCI H460 cells with small hairpin RNA phenocopied the chemosensitizing effect of cambinol (Fig. 3*B*). This result suggests that SIRT1 is the critical cambinol target that mediates its chemosensitizing effects. In further support of this idea, we found that cambinol did not increase etoposide sensitivity in SIRT1−/− MEFs (Fig. 3*C*; ref. 28). Cambinol also sensitized NCI H460 cells to paclitaxel (Fig. 3*A*), indicating that the chemosensitizing effect of cambinol is not limited to DNA-damaging agents. Cambinol promoted G_2 cell cycle arrest in response to etoposide and paclitaxel while having no

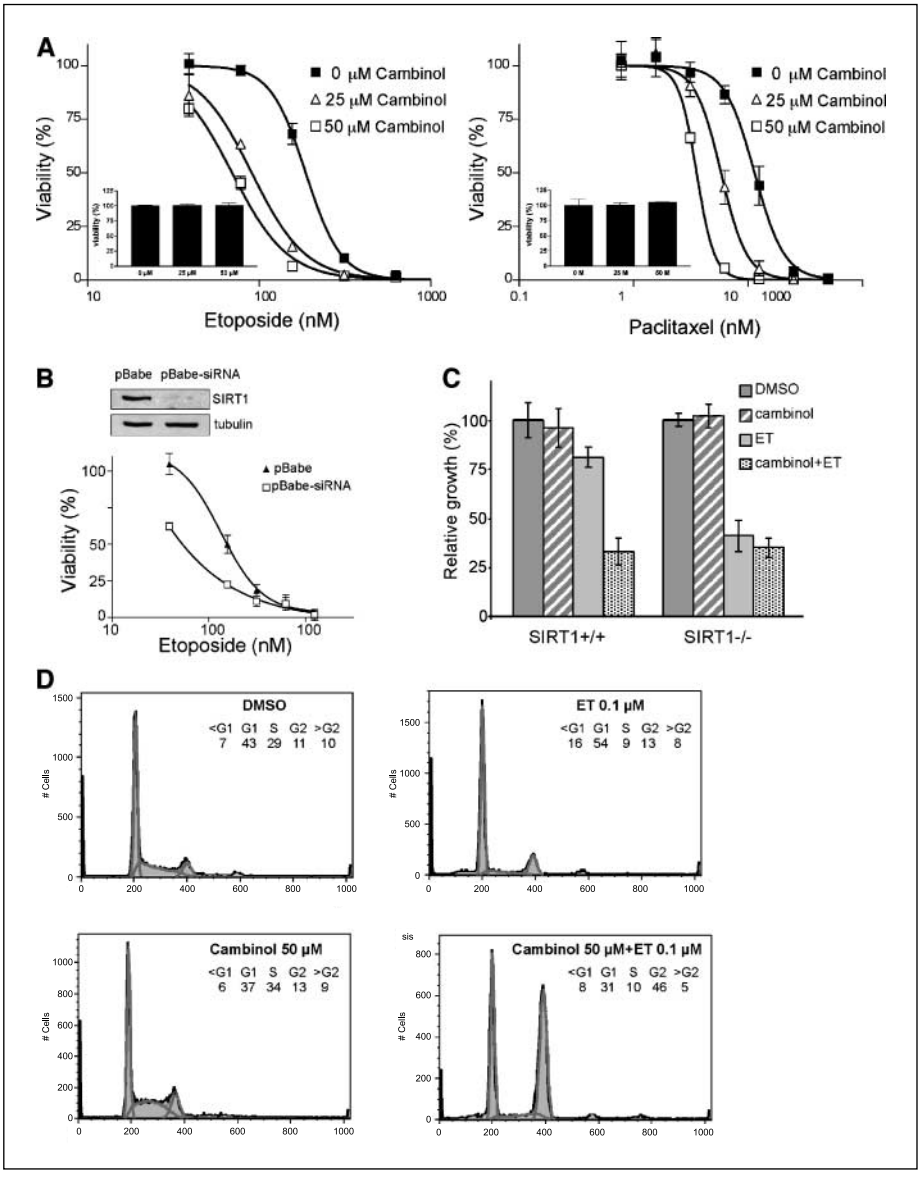

Figure 3. Inhibition of SIRT1 with cambinol sensitizes NCI H460 lung cancer cells to etoposide and paclitaxel and enhances etoposide-induced G_2 arrest. *A,* dose-response curves of etoposide and paclitaxel with and without cambinol. *Insets,* toxicity of cambinol alone. *Points,* cell viability on treatment with combination of cambinol and chemotherapeutic agents (etoposide and paclitaxel), normalized to the viability of cells treated with cambinol alone; *bars,* SD. Experiments were done in triplicates. *B,* down-regulation of endogenous SIRT1 using RNA interference in NCI H460 sensitizes cells to etoposide. *Top,* SIRT1 and (tubulin loading control) immunoblots; *pBabe,* cells infected with empty retroviral vector; *pBabe-siRNA,* SIRT1-specific siRNA-encoding retroviral vector. Etoposide dose-response curve in cells with and without down-regulated SIRT1. The viability of cells is normalized to viability of untreated pBABE and pBabe-siRNA infected cells, 96 ± 3% and 98 ± 2%, respectively. Reduction of endogenous SIRT1 increases sensitivity to etoposide. *C,* cambinol does not chemosensitize SIRT1−/− MEF. SIRT1−/− MEFs and their SIRT+/+ littermate controls were treated with vehicle (DMSO), cambinol alone (50 μmol/L), etoposide alone (*ET*, 100 nmol/L), or a combination of cambinol and etoposide for 72 hours and viable cells were counted. *Y axis,* viability of drug-treated cells relative to vehicle-treated controls. Treatment of SIRT+/+ cells with cambinol increases their sensitivity to etoposide. SIRT1−/− are more sensitive to etoposide than SIRT+/+ cells and cambinol does not increase further their sensitivity to etoposide. *D,* cambinol promotes etoposide-induced G_2 arrest. Flow cytometry DNA analysis of NCI H460 cells treated for 48 hours with DMSO, cambinol, etoposide, and the combination of cambinol and etoposide at indicated concentrations.

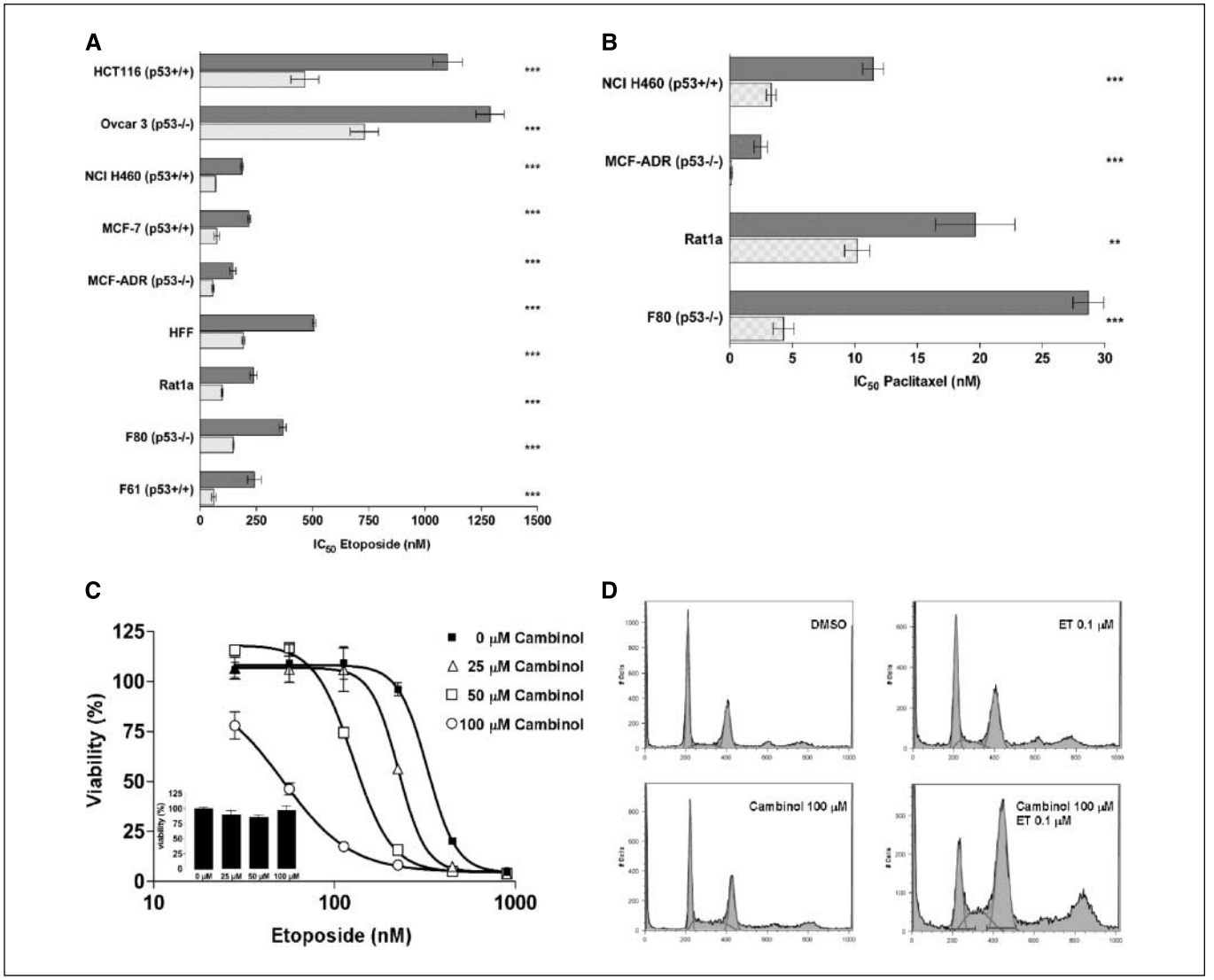

Figure 4. Cambinol sensitizes cells to chemotherapeutic agents in a p53-independent manner. *A,* etoposide IC_{50} values were determined using the [^{3}H]thymidine incorporation assay and normalized to the viability of cells treated with cambinol alone. *Dark gray columns,* IC_{50} of etoposide without cambinol. *Light gray columns,* IC_{50} of etoposide with 50 μmol/L cambinol. *Bars,* SD. Statistical significance was assessed using the two-tailed *t* test. Cambinol reduced the IC_{50} values of etoposide significantly ($P < 0.001$). The viability of cells treated with 50 μmol/L cambinol alone (expressed as percentage of viability in DMSO) was as follows: HCT116, 102%; Ovcar 3, 102%; NCI H460, 101%; MCF-7, 57%; MCF-ADR, 88%; human foreskin fibroblasts, 91%; Rat1a, 94%; F80, 91%; F61, 93%. *B, dark gray columns,* IC_{50} of paclitaxel without cambinol. *Light gray columns,* IC_{50} of paclitaxel with 50 μmol/L cambinol. Cambinol reduced the IC_{50} values of paclitaxel significantly (***, $P < 0.001$; **, $P < 0.01$). The viability of cells treated with 50 μmol/L cambinol alone (expressed as percentage of viability in DMSO) was as follows: NCI H460, 105%; MCF-ADR, 85%; Rat1a, 104%; F80, 94%. Cambinol-induced chemosensitization to etoposide (*C*) and the enhancement of cell cycle arrest (*D*) is independent of p53. *C,* etoposide viability dose-response curves in F80 (p53−/−) MEFs without and with the indicated concentrations of cambinol. *Inset,* viability of cells treated with cambinol alone. *Points,* cell viability on treatment with combination of cambinol and etoposide, normalized to the viability of cells treated with cambinol alone; *bars,* SD. Experiments were done in triplicates. *D,* flow cytometry DNA analysis of F80 (p53−/−) cells treated for 48 hours with DMSO, cambinol, etoposide, and the combination of cambinol and etoposide at indicated concentrations.

significant cell cycle effect on its own (Fig. 3*D* and data not shown).

The cell cycle effects of cambinol and sensitization to etoposide are consistent with the SIRT1 inhibition–mediated acetylation and thus activation of p53. However, the chemosensitizing effect of cambinol was seen consistently, albeit to varying degrees, in all cancer cell lines that we have evaluated (Fig. 4*A* and *B* and data not shown) and the fact that many of the tested cancer lines were deficient in p53 (e.g., MCF-ADR, OVCAR3) suggested that the cambinol chemosensitizing effect is not dependent on an intact p53 pathway. To evaluate the role of p53 in a more defined model, we tested cambinol-induced chemosensitization to etoposide in MEFs derived from p53−/− mice (44). We found that the cambinol-mediated sensitization to etoposide and promotion of etoposide-induced cell cycle arrest was not dependent on p53, as p53-negative MEFs (F80 p53−/−) show a comparable or greater degree of chemosensitization (Fig. 4*A* and *C*) and cell cycle (Fig. 4*D*) arrest relative to p53-positive MEFs. Cambinol chemosensitizing effect was also independent of the K70 or Foxo3a pathways as shown by intact cambinol-induced chemosensitization in chicken lymphoblastic B cell line DT40 lacking Ku70 protein (45) or in Foxo3a-deficient MEFs (ref. 36; Supplementary Fig. S5). The fact that cambinol-induced chemosensitization occurs in the absence of p53, Ku70, and Foxo3a rules out each of these

proteins as the dominant sirtuin deacetylation target that mediates the chemosensitizing effect of cambinol. Based on these findings, we hypothesize that SIRT1 has other relevant targets, in addition to p53, Ku70, and Foxo3a that are important in DNA damage responses and that seem to be present in all cancer cell lines that we have examined.

Antitumor activity of cambinol as a single agent *in vitro* and in a mouse xenograft model. Our initial results suggested that inhibition of cellular SIRT1 and SIRT2 is well tolerated in the absence of other cellular stresses. To evaluate the possibility that sirtuin activity is required for viability in a subset of cancers, we carried out toxicity assays in a larger panel of human cancer cell lines with primary human and rodent fibroblasts as controls. Because of the report that sirtuins deacetylate and regulate the function of transcriptional repressor BCL6 (18), several B cell lines of germinal center origin that express BCL-6 (Fig. 5*A*) were included in the analysis. Cambinol showed most potent activity against Burkitt lymphoma cell lines (Fig. 5*B*). The nontransformed, EBV-immortalized B cells (B1, B2, and B3), that do not express BCL6 (Fig. 5*A*) were not sensitive to cambinol. Cambinol was also less toxic to most of the carcinoma and primary cells (IC_{50} > 60 μmol/L; Fig. 5*B*). Cambinol treatment induced apoptosis in Burkitt lymphoma cells as shown by dose-dependent increase in the proportion of cells with sub-G_1 DNA content (Fig. 5*C*) and further confirmed by Annexin V staining (Supplementary Fig. S6). Treatment of Burkitt lymphoma cells with cambinol did not promote their differentiation along the B-cell lineage, as judged by the lack of appearance of plasma cell surface markers (Supplementary Fig. S7). The SIRT1/SIRT2–inactive cambinol derivative ADS012 (Fig. 1*A* and *B*) containing phenol in place of naphtol was nontoxic to Burkitt lymphoma cells (Fig. 5*D*), suggesting that the toxicity of cambinol in Burkitt lymphoma cells is related to sirtuin inhibition.

We evaluated two possibilities as potential causes for Burkitt lymphoma sensitivity to sirtuin inhibition. We first considered the possible role of sirtuins in the suppression of activation of checkpoint pathways in Burkitt lymphoma cells. In support of this possibility, we noted that the cambinol treatment induced hyperacetylation of p53 in Burkitt lymphoma cells in the absence of any DNA-damaging agent or any other external insult (Fig. 6*A*).

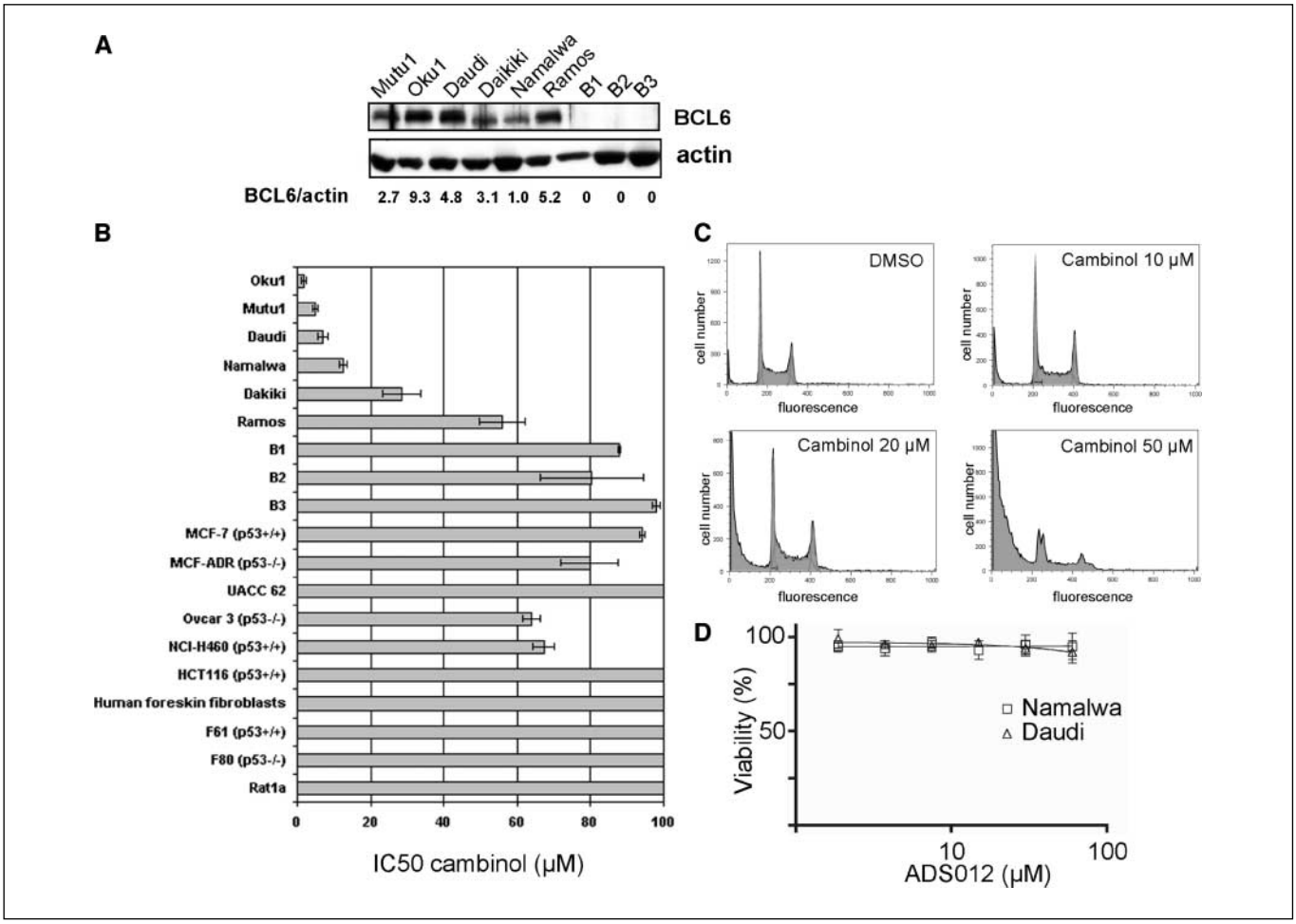

Figure 5. Cambinol is active as a single agent in Burkitt lymphoma cell lines. *A,* Burkitt lymphoma cell lines (Oku1, Mutu1, Daudi, Daikiki, Namalwa, and Ramos) express BCL6, whereas EBV-immortalized B cell lines (B1, B2, and B3) do not express BCL6. BCL6 and actin immunoblots. *B,* IC_{50} measured by [^{3}H]thymidine incorporation in a panel of cell lines. The Burkitt lymphoma cells Oku1, Mutu1, Daudi, Daikiki, and Namalwa are the most sensitive. EBV-immortalized B cells (B1, B2, and B3) and most epithelial cancer and fibroblasts have IC_{50} values >60 to 100 μmol/L. *C,* cambinol induces apoptosis in Burkitt lymphoma cells. DNA content was analyzed by flow cytometry of Namalwa cells treated with the indicated concentrations of cambinol for 48 hours. Sub-G_1 fraction indicates apoptosis. *D,* cambinol derivative ADS012 that lacks sirtuin inhibitory activity is nontoxic in Burkitt lymphoma cell lines. Viability of cells treated for 96 hours with ADS012 is measured using [^{3}H]thymidine incorporation.

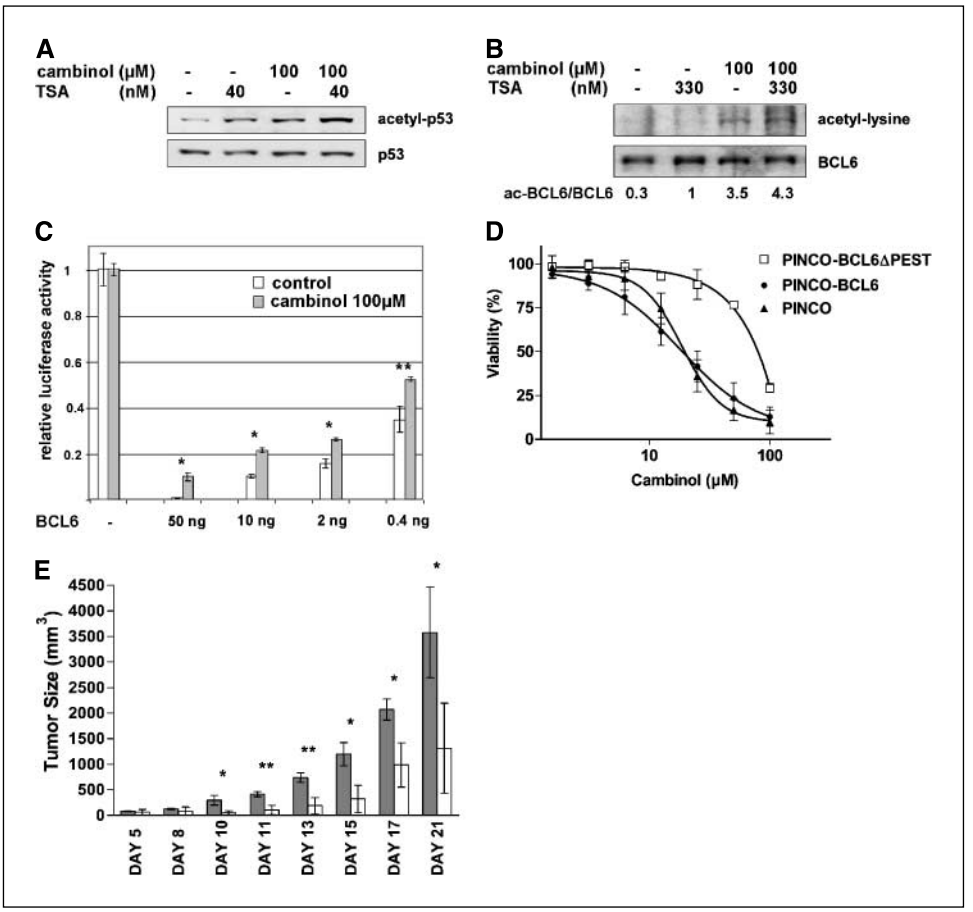

Figure 6. Cambinol induces hyperacetylation of p53 and BCL6 and interferes with BCL6 transcriptional repression. *A,* cambinol and trichostatin A induce hyperacetylation of p53 in Burkitt lymphoma cells. Namalwa cells were incubated with the indicated amounts of deacetylase inhibitors for 5 hours and the cell lysates were analyzed by anti-acetyl-p53 and anti-p53 antibodies. *B,* cambinol induces hyperacetylation of BCL6 in Burkitt lymphoma cells. BCL6 was immunoprecipitated from Ramos cells treated with cambinol and/or trichostatin A for 5 hours. Acetylated and total of BCL6 were analyzed by immunobloting. *C,* cambinol attenuates BCL6 repression function. BCL6 reporter vector with luciferase gene controlled with thymidine-kinase promoter and five GAL4 binding sites (G5TK-pGL2) was transfected into NCI-H460 cells alone or with the vector engineered to express a fusion protein consisting of GAL4 DNA binding domain fused to BCL6, pCDNA3(GAL4)-BCL6 (0.4-50 ng/transfection). *Columns,* luciferase activity measured in transfected cells treated with cambinol (100 μmol/L) or DMSO (control) and normalized to β-galactosidase activity derived from the cotransfected CMV-β-galactosidase vector; *bars,* SD. Experiments were done in triplicates. *, $P < 0.01$; **, $P < 0.05$, two-tailed *t* test. *D,* the nonacetylatable allele of BCL6 confers resistance to cambinol. Namalwa cells were infected with the control retroviral vector containing GFP as a selectable marker (PINCO) or with the BCL6- and BCL6DPEST-expressing vectors (PINCO-BCL6 and PINCO-BCL6DPEST). Pure populations of infected cells were obtained by fluorescence-activated cell sorting using GFP marker and cambinol dose-response curves were generated using [^{3}H]thymidine incorporation assay. The expression of BCL6 and BCL6DPEST was confirmed by Western blot against the hemagglutinin epitope that was used to tag the proteins (data not shown). *E,* response of xenografts of Daudi cells to systemic administration of cambinol to mice. Five days after implantation of cells, cambinol or vehicle was administered systemically (i.v. or i.p.) for 2 weeks (five injections weekly). Cambinol was prepared as 10%/10% ethanol/Cremophore solution to improve solubility. The dose of 100 mg/kg cambinol was the highest dose that could be administered as a single i.v. injection due to limited solubility of the drug. Each group consisted of three animals. Tumor volumes in cambinol (*open columns*) and vehicle treated animals (*solid columns*) of cambinol. **, $P < 0.01$; *, $P < 0.05$, two-tailed *t* test.

Second, we evaluated the possibility that sirtuin inhibition with cambinol alters acetylation status and function of BCL6 oncoprotein. BCL6 is a transcriptional repressor that plays key roles in germinal center formation and in the pathogenesis of a large fraction of B-cell lymphomas. BCL6 function depends on the activity of HDACs and sirtuins (18), as hyperacetylated BCL6 has reduced activity. The critical BCL6 residue subjected to acetylation has been mapped to Lys^{379} (18) and resides within the PEST region involved in control of ubiquitin-mediated degradation (41). We found that cambinol-induced sirtuin inhibition increased BCL6 acetylation (Fig. 6*B*). Consistent with the known effect of BCL6 acetylation on its repression function, we found that cambinol attenuated BCL6-mediated repression in an established BCL6 reporter assay (Fig. 6*C*; ref. 37). These results suggest that treatment with cambinol leads to hyperacetylation of BCL6 and thus abrogation of BCL6 repression function. To better define the role of BCL6 acetylation in cambinol-induced toxicity in Burkitt lymphoma cells, we introduced into Burkitt lymphoma cells an allele of BCL6 that lacks the critical lysine residue subjected to acetylation. This BCL6 allele, *BCL6ΔPEST*, previously characterized in the Dalla-Favera laboratory, is fully functional but cannot be modulated by acetylation (18, 40, 41). Namalwa cells infected with BCL6ΔPEST retroviral expression vector (PINCO-BCL6ΔPEST) are less sensitive to cambinol (IC_{50} > 50 μmol/L) than the cells infected with PINCO control vector (IC_{50} 18 ± 2 μmol/L; Fig. 6*D*) or with the wild-type BCL6 expression vector, PINCO-BCL6 (IC_{50} 19 ± 3 μmol/L). This finding establishes BCL6 as an important sirtuin deacetylation target that mediates cambinol toxicity in Burkitt lymphoma cells. However, we cannot rule out potential effect on the p53 pathway. As Daudi cells are tumorigenic in immunodeficient mice, these cells provided the opportunity to determine if cambinol might be

active in xenografts after systemic administration to mice. Initial studies in Balb-c mice suggested that i.v. doses of 100 mg/kg cambinol are well tolerated. For xenograft studies, 20×10^6 Daudi cells were administered s.c. to the flank region of nonobese diabetic/severe combined immunodeficient mice. After palpable tumors were formed, cambinol, at the dose of 100 mg/kg, or vehicle alone, were administered i.v. into the tail vein or i.p. daily for 2 weeks (five injections weekly). No significant weight loss occurred in cambinol-treated animals relative to controls. Animals were euthanized on day 21 because of the large tumor size in the control group. Treatment with cambinol reduced tumor growth (Fig. 6*E*) relative to mice treated with vehicle alone. These findings suggest that cambinol is active in the xenograft model and that concentrations of cambinol *in vivo* are high enough to obtain the antitumor effect without inducing obvious toxicity to animals.

Discussion

The β-naphthol pharmacophore shared by cambinol and other sirtuin inhibitors, including sirtinol (35) and splitomicin (30, 32), suggests that this group of compounds inhibits NAD-dependent deacetylases in a similar fashion. Competition studies with NAD and peptide substrates show that cambinol is competitive with peptide and noncompetitive with NAD. This finding provides an explanation for several properties of cambinol, including its selectivity among Sir2 family members and low toxicity *in vivo*. The fact that cambinol is competitive with peptide is in agreement with studies of splitomicin-resistant yeast Sir2 mutants (30). Splitomicin-resistant mutants contain point mutations in a small helical domain of Sir2 adjacent to the peptide binding site and distal to the NAD binding site. A single amino acid difference in the small helical domain of yeast Sir2 and its homologue Hst1, was found to underlie the ability of splitomicin to differentiate these two highly related enzymes (31). Cambinol, like splitomicin, discriminates between Sir2 family members as it is selective for SIRT1 and SIRT2. Because splitomicin and cambinol do not affect the NAD binding site, they are not expected to interfere with the function of other Rossman-fold-containing enzymes, including cellular dehydrogenases. Low toxicity is consistent with the lack of off-target activity and is likely related to the mechanism of action of cambinol.

Consistent with the known role of SIRT1 in promoting cell survival, cambinol-induced inhibition of SIRT1 sensitizes cells to chemotherapeutic agents and induced hyperacetylation of known sirtuin targets implicated in stress responses p53, Ku70, and Foxo3a. However, we found that chemosensitization is preserved in cells lacking each of these proteins. This result shows that no single one of these SIRT1 targets plays a dominant role in cambinol-mediated chemosensitization and suggests the presence of other SIRT1-dependent pathways that control resistance to cellular stresses. Other effectors that mediate p53-independent transcription and cell cycle responses upon administration of chemotherapeutic agents include E2F-1 and the p53 family member p73 (46). As p73, E2F1 (47, 48), and several other regulatory proteins [e.g., Rb, nuclear factor-κB (NF-κB), and other forkhead transcription factors; refs. 49, 50] are controlled with reversible acetylation, they present potential targets of SIRT1. In contrast to the effect of SIRT1 on p53, Ku70, and Foxo3a, which promote cell survival, the deacetylation of NF-κB was proposed to enhance NF-κB signaling and thus promote cell death (51). This result suggests that SIRT1 role during stress is complex and that the effect of its inhibition is likely to be cell context specific and determined by the relative importance of the various SIRT1-dependent pathways. Nevertheless, the fact that a large majority of tested cancer cell lines is sensitized with cambinol suggests that the SIRT1-regulated survival pathways exist in most cells and that the net effect of SIRT1 inhibition through these pathways promotes cell death.

Although cambinol sensitized most cells to chemotherapeutic agents, SIRT1/SIRT2 inhibition was well tolerated in the absence of other noxious stimuli. This result is consistent with the specialized role of SIRT1 in promoting cell survival under stress. However, cambinol was toxic in a group of Burkitt lymphoma cell lines in the absence of exogenous stresses, suggesting that sirtuins carry out essential functions in these cells. In support of this idea, we found that β-naphtol pharmacophore modification of cambinol that produces loss of SIRT1/SIRT2 inhibitory activity abolished cambinol toxicity in Burkitt lymphoma cells. The transcriptional repressor BCL6 is an oncoprotein involved in the pathogenesis of germinal center lymphomas, which encompass a large fraction of B-cell lymphomas including Burkitt (52, 53). Recent demonstration that disruption of BCL6 function leads to growth arrest and apoptosis of the BCL6-containing B-lymphoma cells shows that BCL6 pathway is essential for viability of germinal center tumors (54). Three experimental findings support the importance of BCL6 as a relevant sirtuin target that mediates cambinol toxicity in Burkitt lymphoma cells. First, consistent with the known role of sirtuins in deacetylation and function of BCL6, we found that BCL6 is hyperacetylated in Burkitt lymphoma cells on cambinol treatment. Second, cambinol attenuated BCL6 repression activity in heterologous transcription reporter assay. Third, nonacetylatable *BCL6* allele confers resistance to cambinol in Burkitt lymphoma cells. These observations show that interfering with BCL6 function plays an important role in mediating cambinol-induced cell death in Burkitt lymphoma cells. However, the lack of direct correlation between BCL6 level and cambinol toxicity among the Burkitt lymphoma cell lines (e.g., Ramos cells that have the high BCL6 level were the least sensitive to cambinol) suggests the importance of other pathways as mediators of cambinol toxicity in Burkitt lymphoma cells. An additional mechanism for cambinol toxicity, activation of checkpoint pathways, was suggested by the finding that cambinol treatment in Burkitt lymphoma cells induced hyperacetylation of p53 in the absence of any other stressors. Because cellular oncogenes, such as Myc, and external stresses often activate similar pathways (55), it is possible that the role of SIRT1 in suppressing the checkpoint activation in Burkitt lymphoma cells may be analogous to its role in suppressing the activation of checkpoint pathways during external stress in other cell types. Both effects, inactivation of BCL6 function and activation of checkpoint proteins, are likely to be responsible for the antitumor effects of cambinol in Burkitt lymphoma cells. Because BCL6 and cell cycle checkpoint pathways are highly interconnected (41, 56), it may be difficult to dissect the relative contribution of the two proposed pathways.

Our results suggest that sirtuin inhibition may be used as a single modality in tumors, where, similarly to Burkitt lymphoma in our study, sirtuins carry out essential functions. The finding that BCL6 is hyperacetylated in response to cambinol in Burkitt lymphoma cells raises the possibility that other BCL6-expressing

B-cell lymphomas might be sensitive to sirtuin inhibition. Identification of other sirtuin deacetylation targets involved in tumorigenesis and genotoxic stress response has the potential to reveal other tumor contexts where sirtuin inhibition presents a therapeutic opportunity. Our studies suggest that NAD-dependent deacetylases presents a target for cancer therapy and add a novel class of agents to the existing drugs that target protein acetylation.

Acknowledgments

Received 10/6/2005; revised 1/13/2006; accepted 2/8/2006.

Grant support: NIH grants HL04211 and DK56465, Doctors Cancer Foundation, Leukemia and Lymphoma Society (A. Bedalov), and National Cancer Institute grant CA78746 (J.A. Simon).

The costs of publication of this article were defrayed in part by the payment of page charges. This article must therefore be hereby marked *advertisement* in accordance with 18 U.S.C. Section 1734 solely to indicate this fact.

We thank Riccardo Dalla-Favera, Paul Wade, Bob Eisenman, Sara Hook, and Eric Verdin for their gifts of plasmids and antibodies.

References

1. Sterner DE, Berger SL. Acetylation of histones and transcription-related factors. Microbiol Mol Biol Rev 2000;64:435–59.

2. Khochbin S, Verdel A, Lemercier C, Seigneurin-Berny D. Functional significance of histone deacetylase diversity. Curr Opin Genet Dev 2001;11:162–6.

3. Imai S, Armstrong CM, Kaeberlein M, Guarente L. Transcriptional silencing and longevity protein Sir2 is an NAD-dependent histone deacetylase. Nature 2000; 403:795–800.

4. Tanner KG, Landry J, Sternglanz R, Denu JM. Silent information regulator 2 family of NAD-dependent histone/protein deacetylases generates a unique product, 1-*O*-acetyl-ADP-ribose. Proc Natl Acad Sci U S A 2000;97:14178–82.

5. Avalos JL, Celic I, Muhammad S, Cosgrove MS, Boeke JD, Wolberger C. Structure of a Sir2 enzyme bound to an acetylated p53 peptide. Mol Cell 2002;10:523–35.

6. Finnin MS, Donigian JR, Pavletich NP. Structure of the histone deacetylase SIRT2. Nat Struct Biol 2001;8:621–5.

7. Zhao K, Chai X, Marmorstein R. Structure of the yeast Hst2 protein deacetylase in ternary complex with 2′-O-acetyl ADP ribose and histone peptide. Structure (Camb) 2003;11:1403–11.

8. Min J, Landry J, Sternglanz R, Xu RM. Crystal structure of a SIR2 homolog-NAD complex. Cell 2001;105:269–79.

9. North BJ, Verdin E. Sirtuins: Sir2-related NAD-dependent protein deacetylases. Genome Biol 2004;5:224–30.

10. Blander G, Guarente L. The Sir2 family of protein deacetylases. Annu Rev Biochem 2004;73:417–35.

11. Frye RA. Phylogenetic classification of prokaryotic and eukaryotic Sir2-like proteins. Biochem Biophys Res Commun 2000;273:793–8.

12. Vaziri H, Dessain SK, Ng Eaton E, et al. hSIR2(SIRT1) functions as an NAD-dependent p53 deacetylase. Cell 2001;107:149–59.

13. Luo J, Nikolaev AY, Imai S, et al. Negative control of p53 by Sir2α promotes cell survival under stress. Cell 2001;107:137–48.

14. Cohen HY, Lavu S, Bitterman KJ, et al. Acetylation of the C terminus of Ku70 by CBP and PCAF controls Bax-mediated apoptosis. Mol Cell 2004;13:627–38.

15. Brunet A, Sweeney LB, Sturgill JF, et al. Stress-dependent regulation of FOXO transcription factors by the SIRT1 deacetylase. Science 2004;303:2011–5.

16. Araki T, Sasaki Y, Milbrandt J. Increased nuclear NAD biosynthesis and SIRT1 activation prevent axonal degeneration. Science 2004;305:1010–3.

17. Cohen HY, Miller C, Bitterman KJ, et al. Calorie restriction promotes mammalian cell survival by inducing the SIRT1 deacetylase. Science 2004;305:390–2.

18. Bereshchenko OR, Gu W, Dalla-Favera R. Acetylation inactivates the transcriptional repressor BCL6. Nat Genet 2002;32:606–13.

19. Fulco M, Schiltz RL, Iezzi S, et al. Sir2 regulates skeletal muscle differentiation as a potential sensor of the redox state. Mol Cell 2003;12:51–62.

20. Picard F, Kurtev M, Chung N, et al. Sirt1 promotes fat mobilization in white adipocytes by repressing PPAR-γ. Nature 2004;429:771–6.

21. North BJ, Marshall BL, Borra MT, Denu JM, Verdin E. The human Sir2 ortholog, SIRT2, is an NAD dependent tubulin deacetylase. Mol Cell 2003;11:437–44.

22. Schwer B, North BJ, Frye RA, Ott M, Verdin E. The human silent information regulator (Sir)2 homologue hSIRT3 is a mitochondrial nicotinamide adenine dinucleotide-dependent deacetylase. J Cell Biol 2002; 158:647–57.

23. Gu W, Roeder RG. Activation of p53 sequence-specific DNA binding by acetylation of the p53 C-terminal domain. Cell 1997;90:595–606.

24. Matsuyama A, Shimazu T, Sumida Y, et al. *In vivo* destabilization of dynamic microtubules by HDAC6-mediated deacetylation. EMBO J 2002;21:6820–31.

25. Marks PA, Richon VM, Breslow R, Rifkind RA. Histone deacetylase inhibitors as new cancer drugs. Curr Opin Oncol 2001;13:477–83.

26. Sandor V, Bakke S, Robey RW, et al. Phase I trial of the histone deacetylase inhibitor, depsipeptide (FR901228, NSC 630176), in patients with refractory neoplasms. Clin Cancer Res 2002;8:718–28.

27. Piekarz RL, Robey R, Sandor V, et al. Inhibitor of histone deacetylation, depsipeptide (FR901228), in the treatment of peripheral and cutaneous T-cell lymphoma: a case report. Blood 2001;98:2865–8.

28. Cheng HL, Mostoslavsky R, Saito S, et al. Developmental defects and p53 hyperacetylation in Sir2 homolog (SIRT1)-deficient mice. Proc Natl Acad Sci U S A 2003;100:10794–9.

29. McBurney MW, Yang X, Jardine K, et al. The mammalian SIR2α protein has a role in embryogenesis and gametogenesis. Mol Cell Biol 2003;23:38–54.

30. Bedalov A, Gatbonton T, Irvine WP, Gottschling DE, Simon JA. Identification of a small molecule inhibitor of Sir2p. Proc Natl Acad Sci U S A 2001;98:15113–8.

31. Hirao M, Posakony J, Nelson M, et al. Identification of selective inhibitors of NAD^+-dependent deacetylases using phenotypic screens in yeast. J Biol Chem 2003; 278:52773–82.

32. Posakony J, Hirao M, Stevens S, Simon JA, Bedalov A. Inhibitors of Sir2: evaluation of splitomicin analogues. J Med Chem 2004;47:2635–44.

33. Bedalov A, Hirao M, Posakony J, Nelson M, Simon J. NAD-dependent deacetylase Hst1p controls biosynthesis and cellular NAD levels in *Saccharomyces cerevisiae*. Mol Cell Biol 2003;23:7044–54.

34. Posakony J, Hirao M, Bedalov A. Identification and characterization of Sir2 inhibitors through phenotypic assays in yeast. Comb Chem High Throughput Screen 2004;7:661–8.

35. Grozinger CM, Chao ED, Blackwell HE, Moazed D, Schreiber SL. Identification of a class of small molecule inhibitors of the sirtuin family of NAD-dependent deacetylases by phenotypic screening. J Biol Chem 2001;276:38837–43.

36. Castrillon DH, Miao L, Kollipara R, Horner JW, DePinho RA. Suppression of ovarian follicle activation in mice by the transcription factor Foxo3a. Science 2003; 301:215–8.

37. Fujita N, Jaye DL, Geigerman C, et al. MTA3 and the Mi-2/NuRD complex regulate cell fate during B lymphocyte differentiation. Cell 2004;119:75–86.

38. Lamb JR, Goehle S, Ludlow C, Simon JA. Thymidine incorporation is highly predictive of colony formation and can be used for high throughput screening. Biotechniques 2001;30:1118–20.

39. Berenbaum MC. What is synergy? Pharmacol Rev 1989;41:93–141.

40. Niu H, Cattoretti G, Dalla-Favera R. BCL6 controls the expression of the B7-1/CD80 costimulatory receptor in germinal center B cells. J Exp Med 2003;198:211–21.

41. Phan RT, Dalla-Favera R. The BCL6 proto-oncogene suppresses p53 expression in germinal-centre B cells. Nature 2004;432:635–9.

42. Hubbert C, Guardiola A, Shao R, et al. HDAC6 is a microtubule-associated deacetylase. Nature 2002;417: 455–8.

43. Piperno G, LeDizet M, Chang XJ. Microtubules containing acetylated α-tubulin in mammalian cells in culture. J Cell Biol 1987;104:289–302.

44. Lowe SW, Schmitt EM, Smith SW, Osborne BA, Jacks T. p53 is required for radiation-induced apoptosis in mouse thymocytes. Nature 1993;362:847–9.

45. Takata M, Sasaki MS, Sonoda E, et al. Homologous recombination and non-homologous end-joining pathways of DNA double-strand break repair have overlapping roles in the maintenance of chromosomal integrity in vertebrate cells. EMBO J 1998;17:5497–508.

46. Irwin MS, Kondo K, Marin MC, Cheng LS, Hahn WC, Kaelin WGJ. Chemosensitivity linked to p73 function. Cancer Cell 2003;3:403–10.

47. Martinez-Balbas MA, Bauer UM, Nielsen SJ, Brehm A, Kouzarides T. Regulation of E2F1 activity by acetylation. EMBO J 2000;19:662–71.

48. Costanzo A, Merlo P, Pediconi N, et al. DNA damage-dependent acetylation of p73 dictates the selective activation of apoptotic target genes. Mol Cell 2002;9: 175–86.

49. Chan HM, Krstic-Demonacos M, Smith L, Demonacos C, La Thangue NB. Acetylation control of the retinoblastoma tumour-suppressor protein. Nat Cell Biol 2001; 3:667–74.

50. Chen LF, Fischle W, Verdin E, Greene WC. Duration of nuclear NF-κB action regulated by reversible acetylation. Science 2001;293:1653–7.

51. Yeung F, Hoberg JE, Ramsey CS, et al. Modulation of NF-κB-dependent transcription and cell survival by the SIRT1 deacetylase. EMBO J 2004;23:2369–80.

52. Sanchez-Beato M, Sanchez-Aguilera A, Piris MA. Cell cycle deregulation in B-cell lymphomas. Blood 2003;101: 1220–35.

53. Ye BH, Lista F, Lo Coco F, et al. Alterations of a zinc finger-encoding gene, BCL-6, in diffuse large-cell lymphoma. Science 1993;262:747–50.

54. Polo JM, Dell'oso T, Ranuncolo SM, et al. Specific peptide interference reveals BCL6 transcriptional and oncogenic mechanisms in B-cell lymphoma cells. Nat Med 2004;10:1329–35.

55. Nilsson JA, Cleveland JL. Myc pathways provoking cell suicide and cancer. Oncogene 2003;22:9007–21.

56. Shvarts A, Brummelkamp TR, Scheeren F, et al. A senescence rescue screen identifies BCL6 as an inhibitor of anti-proliferative p19(ARF)-p53 signaling. Genes Dev 2002;16:681–6.